Mesenchymal Stem Cell–Derived Small Extracellular Vesicles Promote Neuroprotection in a Genetic DBA/2J Mouse Model of Glaucoma

Ben Mead,[1,2] Zubair Ahmed,[2] and Stanislav Tomarev[1]

[1]Section of Retinal Ganglion Cell Biology, Laboratory of Retinal Cell and Molecular Biology, National Eye Institute, National Institutes of Health, Bethesda, Maryland, United States
[2]Neuroscience and Ophthalmology, Institute of Inflammation and Ageing, College of Medical and Dental Sciences, University of Birmingham, Birmingham, United Kingdom

Correspondence: Ben Mead, Section of Retinal Ganglion Cell Biology, Laboratory of Retinal Cell and Molecular Biology, National Eye Institute, National Institutes of Health, Bethesda, MD 20892, USA; ben.mead@nih.gov.
Stanislav Tomarey, Section of Retinal Ganglion Cell Biology, Laboratory of Retinal Cell and Molecular Biology, National Eye Institute, National Institutes of Health, Bethesda, MD 20892, USA; tomarevs@nei.nih.gov.

ZA and ST are joint senior authors.

Submitted: July 18, 2018
Accepted: October 14, 2018

Citation: Mead B, Ahmed Z, Tomarev S. Mesenchymal stem cell–derived small extracellular vesicles promote neuroprotection in a genetic DBA/2J mouse model of glaucoma. *Invest Ophthalmol Vis Sci*. 2018;59:5473–5480. https://doi.org/10.1167/iovs.18-25310

Purpose. To determine if bone marrow-derived stem cell (BMSC) small extracellular vesicles (sEV) promote retinal ganglion cell (RGC) neuroprotection in the genetic DBA/2J mouse model of glaucoma for 12 months.

Methods. BMSC sEV and control fibroblast-derived sEV were intravitreally injected into 3-month-old DBA/2J mice once a month for 9 months. IOP and positive scotopic threshold responses were measured from 3 months: IOP was measured monthly and positive scotopic threshold responses were measured every 3 months. RGC neuroprotection was determined in wholemounts stained with RNA binding protein with multiple splicing (RBPMS), whereas axonal damage was assessed using paraphenylenediamine staining.

Results. As expected, DBA/2J mice developed chronic ocular hypertension beginning at 6 months. The delivery of BMSC sEV, but not fibroblast sEV, provided significant neuroprotective effects for $RBPMS^+$ RGC while significantly reducing the number of degenerating axons seen in the optic nerve. BMSC sEV significantly preserved RGC function in 6-month-old mice, but provided no benefit at 9 and 12 months.

Conclusions. BMSC sEV are an effective neuroprotective treatment in a chronic model of ocular hypertension for 1 year, preserving RGC numbers and protecting against axonal degeneration.

Keywords: glaucoma, DBA/2J, mesenchymal stem cells, extracellular vesicles, exosomes, retinal ganglion cells

Glaucoma is a leading cause of irreversible blindness and is characterized by the degeneration of retinal ganglion cells (RGC) and their axons. The most common type of glaucoma is referred to as primary open-angle glaucoma, and its critical risk factors include ocular hypertension, genetic predisposition, and aging.[1] Lowering IOP is currently the only treatment option available, but it remains ineffective in many patients.[2]

Current research focuses on the development of neuroprotective strategies to prevent RGC death. Mesenchymal stem cells (MSCs), a multipotent stromal cell, are currently being tested in clinical trials due to having demonstrated efficacy in a multitude of retinal disease models (reviewed in Ref. 3).[4–7] Their mechanism of action was shown to be paracrine mediated through the secretion of neurotrophic factors such as nerve growth factor, brain-derived neurotrophic factor,[8] and platelet-derived growth factor,[9] and more recently, exosomes.[10,11]

Exosomes are extracellular vesicles that are formed within multivesicular bodies and released into the extracellular space upon plasma membrane fusion.[12] Exosomes contain miRNA, mRNA, lipids, and proteins, and these contents are delivered into the cytoplasm upon fusion with a recipient cell.[13] The delivered mRNA is then translated by the recipient cell, whereas miRNA modulates gene expression. Thus, exosomes are a potential novel cell communication mechanism. Microvesicles, another class of extracellular vesicles, are formed instead via outward budding of the plasma membrane. Exosomes range between 40 and 150 nm, whereas microvesicles are found ranging from 100 to 1000 nm; however, these values vary greatly between studies, with some using the term "exosome" to encompass any extracellular vesicle isolated, and others only referring to extracellular vesicles that pass through a 220 nm filter. As a result of the heterogenous nature of the vesicle preparation, small extracellular vesicle (sEV) is a more accurate term and is used throughout the rest of the article.

MSC sEV have shown therapeutic efficacy in several disease models including traumatic brain injury, stroke, and Alzheimer's disease (reviewed in Ref. 14). MSC sEV were shown to localize specifically to the injured region of the spinal cord and modulate M2 macrophages[15] as well as direct the polarization of macrophages from M1 to a M2 phenotype.[16] In many cases, the mechanism of therapeutic action for BMSC sEV appears to be through the delivery of miRNA. For example, subcutaneous delivery of MSC sEV promoted improvements in angiogenesis

and cardiac function through miRNA-mediated mechanisms in a mouse model of myocardial infarction.[17] In a rat stroke model, intravenous administration of MSC sEV and the delivery of miRNA to neurons and astrocytes improved functional recovery[18] as well as the formation of neurons and oligodendrocytes and the suppression of phosphatase and tensin homolog (PTEN) signaling.[19] Intravenous administration of sEV isolated from BMSC into rodent models of spinal cord injury promoted a reduction in cellular apoptosis and inflammation and an improvement in locomotor function.[15,16,20] The neuroprotective efficacy of BMSC sEV on RGC after optic nerve crush or ocular hypertension/glaucoma[10,11] as well as their neuritogenic efficacy on cortical cells[21] were attenuated if sEV miRNA were rendered dysfunctional through the knockdown of argonaute-2 (AGO2) prior to sEV isolation. AGO2 knockdown abrogates miRNA biogenesis, function, and loading into vesicles as well as allows their degradation.[22,23] Several miRNA have been identified as particularly abundant in BMSC sEV[10] in comparison to sEV derived from fibroblast, which are not RGC neuroprotective.[9]

We have previously demonstrated that BMSC sEV promote neuroprotection in two short-term models of glaucoma: a laser model and a microbead model.[10] Delivery of the sEV into the vitreous of rats promoted significant survival of RGC even when injected once a month in a micro bead model during the course of 2 months or a single injection in a laser model during the course of 3 weeks. For future clinical application of exosomes, it is important to test whether exosomes can provide long-term neuroprotection in a chronic model of glaucoma, such as in the DBA/2J genetic mouse model of glaucoma, in which a prolonged rise in IOP occurs. Thus, the purpose of this study is to demonstrate BMSC sEV efficacy in a long-term glaucoma model using a monthly treatment regime previously shown to be sufficient.

Methods

Animals

A total of 60 adult, female, 3-month-old DBA/2J mice (Jackson Laboratories, Bar Harbor, ME, USA) were maintained in accordance with guidelines described in the ARVO Statement for the Use of Animals in Ophthalmic and Vision Research using protocols approved by the National Eye Institute Committee on the Use and Care of Animals. Female mice were chosen as they develop ocular hypertension sooner and to a greater degree than males.[24]

Animals were kept at 21°C/55% humidity under a 12-hour light/dark cycle, were given food/water ad libitum, and were under constant supervision from trained staff. Animals were euthanized by rising concentrations of CO_2 before dissection of retinae and optic nerves.

Materials

All reagents were purchased from Sigma (Allentown, PA, USA) unless otherwise specified.

BMSC Cultures

Human cluster of differentiation 29 $(CD29)^+/CD44^+/CD73^+/CD90^+/CD45^-$ BMSC (confirmed by supplier; Lonza, Walkersville, MD, USA) from 3 pooled donors were cultured in Dulbecco's modified eagle media (DMEM)/1% penicillin/streptomycin/10% exosome-depleted fetal bovine serum (Thermo Fisher Scientific, Cincinnati, OH, USA). Cell cultures were maintained at 37°C in 5% CO_2 with medium changed every 3 days and cells passaged with 0.05% trypsin/EDTA when 80% confluent. Human dermal fibroblasts (Lonza), which was used as control cells were grown in the above conditions and used as a control. For all experiments, BMSC and dermal fibroblasts were used at passages 2 to 5.

Exosome/sEV Isolation and Quantification

Exosomes were isolated from BMSC and fibroblasts using a polyethylene glycol (PEG) solution (ExoQuick-TC; System Biosciences, Mountain View, CA, USA) per the manufacturer's instructions. Briefly, conditioned medium was centrifuged at 3000*g* for 15 minutes to remove cells and debris, incubated with ExoQuick reagent overnight at 4°C (1:10 ratio with medium), and centrifuged at 1500*g* for 15 minutes before resuspension of the exosome pellet in sterile phosphate-buffered saline (sPBS). The exosome preparation is passed through a 0.22 μm filter to remove any large extracellular vesicles (microvesicles and apoptotic bodies). Because PEG precipitation techniques are expected to yield some nonexosomal vesicles in the preparation, we thus refer to the exosomes used in this study as sEV. The sEV were characterized by their positive staining for the exosome/microvesicle markers Syntenin-1 and CD63 and negative staining for high/low density lipoprotein markers apolipoprotein A-1 (ApoA1) and apolipoprotein B (ApoB) using Western blot as previously detailed and reported.[10] To ensure a consistent delivery amount, sEV were quantified as detailed previously using a NanoSight LM10 instrument (Malvern, Worcester, MA, USA).[10] Briefly, for each sample we captured three videos and analyzed them at a detection threshold of two 12.9- to 13.1-pix maximum jump size, automatic blur size, and slider gain at 80 and with a total of 567 frames per video.

In Vivo Experimental Design

A total of 60 DBA/2J mice were separated into one of the following three groups: Group 1 consisted of 20 untreated mice; Group 2 consisted of 20 mice injected monthly with BMSC sEV; Group 3 consisted of 20 mice injected monthly with fibroblast sEV. Experiments began with 3-month-old mice, and they were euthanized at 12 months. A total of 6 mice died toward the end of the experiment, likely due to their old age in combination with anesthesia. DBA/2J mice are known to suffer from colony-specific problems including heart calcifications and thoracic cavity malformations, which are expected to lead to sudden death in a number of animals before the study concludes.[25]

The group with the smallest final count was 17 mice, and the other two groups thus provided 17 mice randomly from their cohort to maintain consistency. Because each eye develops ocular hypertension independent of the contralateral eye,[25] they are thus treated as independent samples[24] resulting in 34 per group. RGC/axonal survival was assessed histologically whereas function was measured via electroretinography (ERG). Optical coherence tomography was not performed as images were of extremely poor quality, making analysis unfeasible in aged DBA/2J mice due to the iris atrophy and irregularly shaped pupil that was not amenable to tropicamide-mediated dilation.[25] Oculomotor response testing was not conducted as DBA/2J mice show no response to these tests.[26]

Intraocular Pressure Recording (IOP)

IOP were recorded for all mice using a Tonolab rebound tonometer (Colonial Medical Supply, Franconia, NH, USA). IOP was recorded under isoflurane-induced anesthesia between 8 and 11 AM, sampled 18 times, and averaged for each individual recording. Recordings were performed monthly from age 3 to 12 months and were taken just prior to the monthly intravitreal

(ivit) injection. It is worth noting that DBA/2J mice are known to develop corneal calcifications, making tonometry recording of IOP unreliable.[25] Indeed, previous studies demonstrate great variation between IOP values recorded by tonometry versus invasive measurements. Care was taken to avoid recording IOP in obvious calcified regions while ensuring the probe point of contact was perpendicular to the cornea; however, without available invasive measuring techniques it can be assumed reliability is inversely proportional to the age of the mice.

Ivit Delivery of sEV

Under isoflurane-induced anesthesia, sEV were injected into the vitreous just posterior to the limbus using glass micropipettes. A 2 µl volume of sPBS loaded with 1×10^9 sEV was injected slowly, and the needle was retracted only after a 1-minute delay to minimize backflow. The concentration was chosen based on our previous studies[10,11] that demonstrated efficacy with the volume and concentration adapted for the mouse vitreous volume. Injections were performed once a month from 3 to 12 months.

ERG Measurements of the Positive Scotopic Threshold Response

ERG was recorded using the Espion Ganzfeld full field system (Diagnosys LLC, Lowell, MA, USA) on 3-month-old mice, before any detectable ocular hypertension or functional decline,[24,25,27] and on mice aged 6, 9, and 12 months, when RGC function is expected to deteriorate. Mice were dark adapted for 12 hours and prepared for ERG recording under dim red light (>630 nm). Anesthesia was induced with intraperitoneal injection of ketamine/xylazine, and the eyes were dilated with tropicamide. Scotopic flash ERG was recorded from −5.5 log (cd s) m^{-2} to 1.0 log (cd s) m^{-2} in 0.5 log unit increments. ERG traces were analyzed using in built Espion software and the amplitude (with respect to baseline) was used as a measure of mouse visual function. Traces at a light intensity of −5.0 log (cd s) m^{-2} were chosen for analysis as they produced a clean, unambiguous positive scotopic threshold response (pSTR) at approximately 100 milliseconds after stimulus, of which the peak amplitude was recorded. Although it is possible that corneal calcifications may have affected the RGC traces, it is expected this effect will be universal for all groups and equally, we were still able to measure pSTR in mice aged 12 months. All readings and analysis were performed by an individual masked to the treatment groups.

Tissue Processing

Mice were euthanized at 12 months by rising concentration of CO_2 and immediately perfused intracardially with 4% paraformaldehyde in PBS. The eyes were enucleated and retinae dissected and immersion postfixed in 4% paraformaldehyde for 1 hour at 4°C. Optic nerves were dissected, cryopreserved in 10%, 2%0, and 30% sucrose solution in PBS for 24 hours at 4°C. Optic nerves were embedded in optimal cutting temperature embedding medium (VWR International, Inc., Bridgeport, NJ, USA) in peel-away mold containers (VWR International, Inc.) and stored at −80°C. Optic nerves were coronally sectioned on a CM1860 Cryostat microtome (Leica Microsystems, Inc., Bannockburn, IL, USA) at −20°C at a thickness of 5 µm, mounted on positively charged glass slides (Superfrost Plus, Fisher Scientific, Pittsburgh, PA, USA), and stored at −80°C until required.

RGC Counts in Retinal Wholemounts

Retinal wholemounts were permeabilized by immersion in 0.5% Triton X-100 in PBS for 15 minutes at −70°C and washed in fresh Triton X-100 for a further 15 minutes before incubation with primary antibody diluted in wholemount antibody diluting buffer (2% bovine serum albumin, 2% Triton X-100 in PBS) overnight at 4°C. The following day, wholemounts were washed for 3 × 10 minutes in PBS and incubated with secondary antibodies in wholemount antibody diluting buffer for 2 hours at room temperature. After 2 hours, retinae were washed for 3 × 10 minutes in PBS and mounted vitreous side up on Superfrost Plus glass slides, facilitated by 4 equidistant cuts into the peripheral retina. The slides were allowed to air dry before mounting in Vectorshield medium (Vector Laboratories, Peterborough, UK) and applying cover slips. The antibodies used are detailed in the Table.

Table. Antibodies Used in Immunohistochemistry (IHC) and Western Blot (WB)

Antigen	Dilution	Supplier	Catalogue No.
RBPMS	1:500 (IHC)	Thermo Fisher	#ABN-1376
Syntentin-1	1:1,000 (WB)	Abcam	#Ab133267
CD63	1:1,000 (WB)	System Bio	#Exoab-CD63-A1
ApoA1	1:1,000 (WB)	Abcam	#ab7613
ApoB	1:1,000 (WB)	Abcam	#ab20737
HSC70	1:5,000 (WB)	Santa Cruz	#sc-7298
Mouse IgG HRP	1:2,000 (WB)	GE Healthcare	#NA-931
Guinea pig IgG 546	1:400 (IHC)	Thermo Fisher	#A-11074
Mouse IgG HRP	1:2,000 (WB)	GE Healthcare	#NA-931
Rabbit IgG HRP	1:10,000 (WB)	Cell Signalling	#7074

RBPMS, RNA-binding protein with multiple splicing; CD63, cluster of differentiation 63; ApoA1, apolipoprotein A-1; ApoB, apolipoprotein B; HSC70, heat shock cognate 71 kDa protein; IgG, immunoglobulin; HRP, horseradish peroxidase.

Retinal wholemounts were imaged using a Z1 Imager epifluorescent microscope equipped with an Axiocam HRc camera (Carl Zeiss, Inc., Thornwood, NY, USA) and RNA binding protein with multiple splicing $(RBPMS)^+$ cells were counted in three 0.33 mm^2 regions per retinal quadrant at 0.5, 1, and 1.5 mm from the optic nerve head. Counts were conducted manually by an individual masked to the treatment group. The mean number of RGC/image was derived from the 12 images, which made up 8.3% of the total retina (16 mm^2)[28] and was used to calculate RGC/mm^2 with each group consisting of 34 retinae from 17 mice.

Glaucomatous Damage Scaling in Optic Nerve Section

Glaucomatous damage in the optic nerve was assessed as previously described.[24,29,30] Briefly, optic nerves were stained in 1% paraphenylenediamine in 1:1 propanol/methanol for 30 minutes at room temperature, washed in ethanol, and allowed to air-dry before being mounted in Permount (Thermo Fisher Scientific). Paraphenylenediamine darkly stains the axoplasm of damaged axons and optic nerves were graded as mild, moderate, or severe damage by two investigators masked both from the treatment group as well as each other's grades. Approximately 20 sections were analyzed per optic nerve. The grading scale followed previous guidelines,[24,29] but briefly, mild represents optic nerves with less than 5% of damaged axons and no gliosis, moderate represents optic nerves with 5% to 30% axonal loss and early gliosis, and severe represents optic nerves with more than 50% axonal loss and prominent gliosis. Because there is overlap, a third masked investigator was used if the initial two investigators disagreed on the grading.

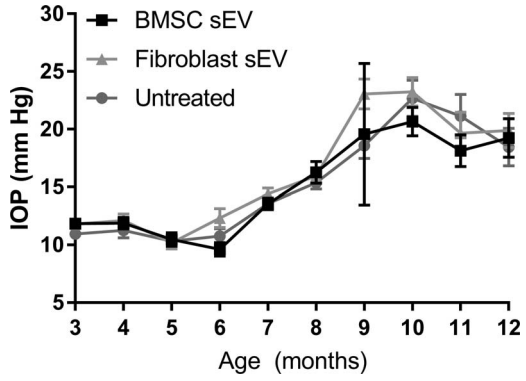

FIGURE 1. IOP measurements in DBA/2J mice. Mean (± SEM) IOP (mm Hg) of untreated animals and animals receiving *ivit* injection of BMSC- or fibroblast-derived sEV. No significant difference ($P > 0.05$) between untreated and experimental groups was found.

Statistics

All statistical tests were performed using SPSS 17.0 (IBM SPSS, Inc., Chicago, IL, USA), and data are presented as mean ± standard error of the mean with graphs constructed using Graphpad Prism 7.01 (Graphpad Prism, La Jolla, CA, USA). The Shapiro-Wilkes test was used to ensure all data were normally distributed before parametric testing using a one-way analysis of variance with a Tukey post-hoc test. Graded optic nerves were compared using Fisher's exact test (2 × 3). Statistical differences were considered significant at P values < 0.05.

RESULTS

DBA/2J Mice Spontaneously Develop Ocular Hypertension

DBA/2J mice maintained normal IOP (10–12 mm Hg) between 3 and 6 months (Fig. 1). At 7 months, IOP increased spontaneously to 13.6 ± 0.5 mm Hg, 13.5 ± 0.5 mm Hg, and 14.4 ± 0.5 mm Hg in untreated, BMSC-sEV-treated, and fibroblast-sEV-treated DBA/2J mice, respectively. By 12 months, IOP increased to 18.4 ± 1.6 mm Hg, 19.3 ± 1.7 mm Hg, and 19.9 ± 1.5 mm Hg in untreated, BMSC-sEV-treated, and fibroblast-sEV-treated DBA/2J mice, respectively. IOP did not significantly differ between the three groups at any age, suggesting that BMSC/fibroblast sEV do not affect IOP in DBA/2J mice.

BMSC sEV Are Neuroprotective in DBA/2J Mice

Quantification of the number of RBPMS$^+$ RGC at 12 months in retinal wholemounts of BMSC-sEV-treated DBA/2J mice (962 ± 116 RGC/mm^2) was significantly higher ($P < 0.001$) than those of fibroblast-sEV-treated mice (268 ± 72 RGC/mm^2) or untreated mice (259 ± 106 RGC/mm^2; Fig. 2). Therefore, BMSC sEV protect 3.7-fold greater numbers of RBPMS$^+$ RGC compared to untreated mice and demonstrates that BMSC sEV are RGC neuroprotective in DBA/2J mice.

BMSC sEV Prevent RGC Functional Decline at 6 Months, but Not 9 or 12 Months

The amplitude of the pSTR was 47.3 ± 2.1 μV in DBA/2J mice aged 3 months (Fig. 3). By 6 months, pSTR amplitude in BMSC-sEV-treated DBA/2J mice had decreased (33.2 ± 3.0 μV) but remained significantly higher than that in fibroblast-sEV-treated mice (22.9 ± 1.8 μV) or untreated mice (26.3 ± 2.4 μV). By 9 and 12 months, pSTR amplitudes in BMSC-sEV-treated (24.9 ± 2.4 μV and 19.7 ± 2.6 μV, respectively), fibroblast-sEV-treated (20.5 ± 2.7 μV and 15.6 ± 3.1 μV, respectively), and untreated (18.5 ± 2.2 μV and 16.1 ± 3.2 μV, respectively) DBA/2J mice had decreased further, but there was no longer a significant difference between groups. These results demonstrate that BMSC sEV prevent the early decline in RGC function, but cannot prevent later decline in RGC function in DBA/2J mice.

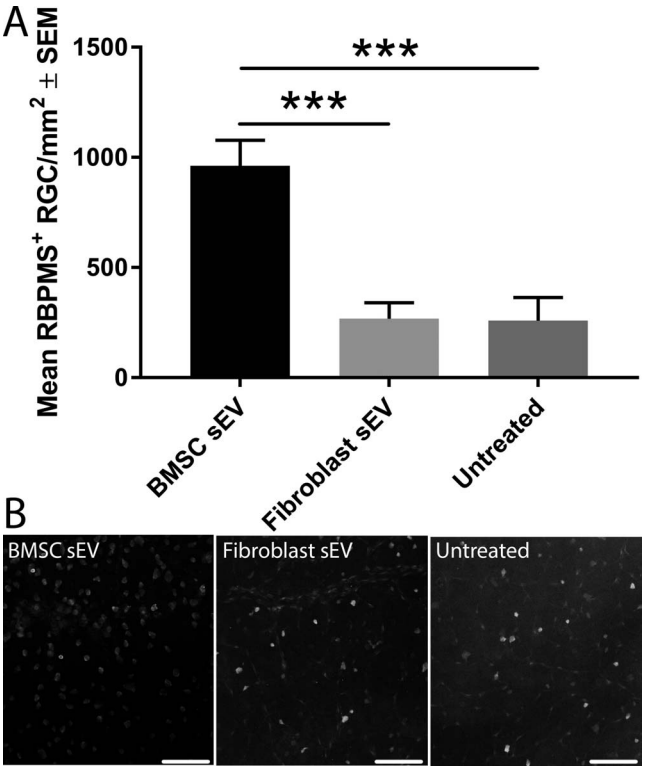

FIGURE 2. Surviving RBPMS$^+$ RGC counts in DBA/2J mice. (**A**) Quantification of the mean (± SEM) number of surviving RBPMS$^+$ RGC in 12-month-old DBA/2J mice with or without *ivit* injection of BMSC- or fibroblast-derived sEV. *Asterisks* indicate significant difference between groups ($P < 0.001$). (**B**) Representative images of RBPMS$^+$ RGC from immunohistochemically stained retinal wholemounts (*scale bar*: 100 μm).

Axonal Degeneration Data

The distribution of optic nerve damage, graded as mild, moderate, and severe, was significantly ($P < 0.01$) skewed more to the severe grading in untreated 12-month-old DBA/2J mice (12%, 22%, 66%, respectively) and mice treated with fibroblast-derived sEV (18%, 24%, 58%, respectively) compared to BMSC-derived-sEV treated mice (33%, 37%, 40%, respectively; Fig. 4). These results suggest that BMSC sEV reduces axonal damage in DBA/2J mice.

DISCUSSION

The present study demonstrates that BMSC sEV do not affect the development of spontaneous ocular hypertension in the DBA/2J genetic mouse model of glaucoma, but protect RBPMS$^+$ RGC from death. The number of degenerating axons in the optic nerve was also significantly diminished after BMSC sEV treatment; however, RGC function deteriorated in all three groups with BMSC sEV only providing a modest significant effect at 6 months.

Investigative Ophthalmology & Visual Science

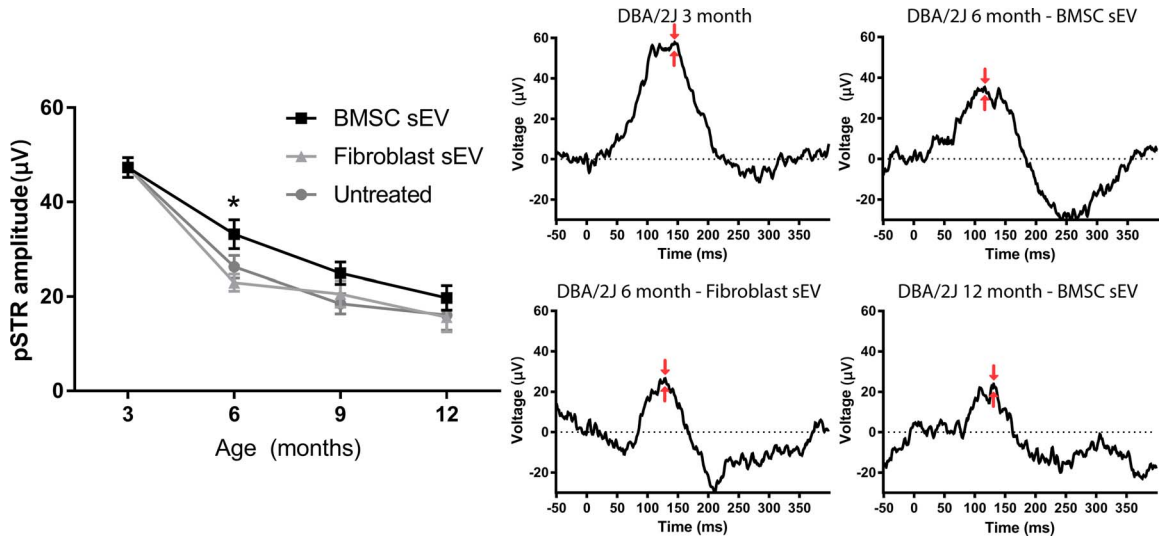

FIGURE 3. ERG measurements of pSTR in DBA/2J mice. (*Left*) Mean (± SEM) amplitude (μV) of pSTR measured by ERG at 3- (untreated healthy baseline), 6- , 9-, and 12-month-old DBA/2J mice with or without *ivit* injection of BMSC- or fibroblast-derived sEV. *Asterisk* indicates significant difference between BMSC-derived sEV treated mice and fibroblast-derived sEV treated/untreated mice ($P < 0.05$). (*Right*) Representative traces of pSTR; *red arrows* indicate the peak amplitude that was measured.

DBA/2J mice are a mouse model of glaucoma, specifically pigmentary glaucoma. Mutations in tyrosinase-related protein 1 and glycosylated protein nmb lead to iris stromal atrophy and iris pigment dispersion, respectively.[31] A buildup of pigment and cell debris in the trabecular meshwork overtime attenuates drainage of aqueous humor, leading to a chronic rise in IOP. Because DBA/2J mice are a mouse strain that spontaneously develop ocular hypertension, they avoid complications arising in other glaucoma models that require physical interventions to elevate IOP. These complications include inflammatory response to injections, lasers, and sutures; short duration elevations in IOP; and an ocular hypertension detached from the effects of age unlike what is seen in humans. A meta-analysis of 1400 DBA/2J mice demonstrated that the initial significant IOP elevation begins at 6 months and peaks at 10 to 12 months.[24] An analysis of 772 nerves demonstrates that 10% to 20% of nerves show a degenerative phenotype at 6 months, whereas at 12 months, 60% to 80% of optic nerves were degenerated. At 16 to 19 months, 80% of optic nerves were degenerated.

Because pressure is uniform throughout the eye, it might be expected that RGC die uniformly, but this is not what is seen.[32] RGC display fan-shaped death, narrow at the optic head with the zone devoid of RGC widening as it radiated out to the periphery.[32,33] This is seen in the human condition, likely due to the compression of axonal bundles as they move through the lamina cribrosa. Although lacking a lamina cribrosa, mice do have a glial component that could elicit similar effects.[34,35] Distinguishing through morphological differences, larger RGC subtypes appear selectively resistant,[32] which is similar to other glaucoma and optic nerve injury models,[36,37] although limited studies exist to make strong conclusions. Thus, as in the human condition, DBA/2J mice display an age-related rise in IOP, a delay between the ocular hypertension and the degeneration of RGC and their axons, and finally, a sectorial, nonuniform pattern of death.

Clinical trials are already ongoing for the use of BMSC as a treatment for several ocular diseases (reviewed in Ref. 3). Two clinical trials have published reports on the efficacy and safety of MSC sEV. The first demonstrated that systemic delivery of MSC sEV improved kidney function and reduced inflammation even 1 year after the treatment was delivered.[38] The second showed that delivery of MSC sEV into a patient with steroid refractory graft-versus-host disease suppressed proinflammatory cytokine secretion and reduced symptoms.[39]

Exosomes offer significant potential advantages over cell therapy. First, because they are nondividing, they can be more accurately dosed. They also likely avoid many of the complications associated with transplanting dividing cells into the eye including the retinal detachment and ocular hypertension reported in three patients receiving intravitreal adipose-derived MSC and who subsequently went blind.[40] Following isolation, sEV can be stored for more than 6 months at −80C° and also 2 weeks at 4°C without loss of miRNA quantity or function.[41]

Although the present study was not aimed at elucidating the neuroprotective mechanism of BMSC sEV on RGC, our previous studies are suggestive of a role for miRNA.[10] Because PEG precipitation isolates other vesicles along with exosomes (hence our use of the term *sEV*) and other nonvesicle structures, we must take care in drawing mechanistic conclusions. For example, miRNA have been found associated with protein aggregates (independent of sEV)[42] as well as virus particles,[43] both of which are constituents of the PEG precipitation along with sEV. Another negative effect of PEG precipitation is that, although producing large yields of sEV, the process can damage exosomes and impact on their biological activity as well as the activity of their protein/nucleic acid cargo.[44] Despite similar neuroprotective efficacy in PEG-isolated and ultracentrifugation-isolated BMSC sEV,[11] we cannot discount the fact that a suboptimal dose was being injected into DBA/2J mice due to activity deficits associated with the PEG isolation technique.

We observed a significant decline in RGC function as measured by flash ERG and recording of the pSTR amplitude. pSTR amplitude decreased from 47 μV at 3 months to 16 μV at 12 months. A previous study demonstrated similar functional decline in female DBA/2J with pSTR amplitude decreasing from 60 μV to 20 μV from 3 to 12 months.[45] A second study showed a larger decline in pSTR, from 100 μV at 3 months to 70 μV, 50 μV, and 25 μV at 6, 9, and 12 months, respectively.[25] The likely reason larger amplitudes were seen in the referenced study compared to our present study are because of the higher flash intensity used by the authors that would have subse-

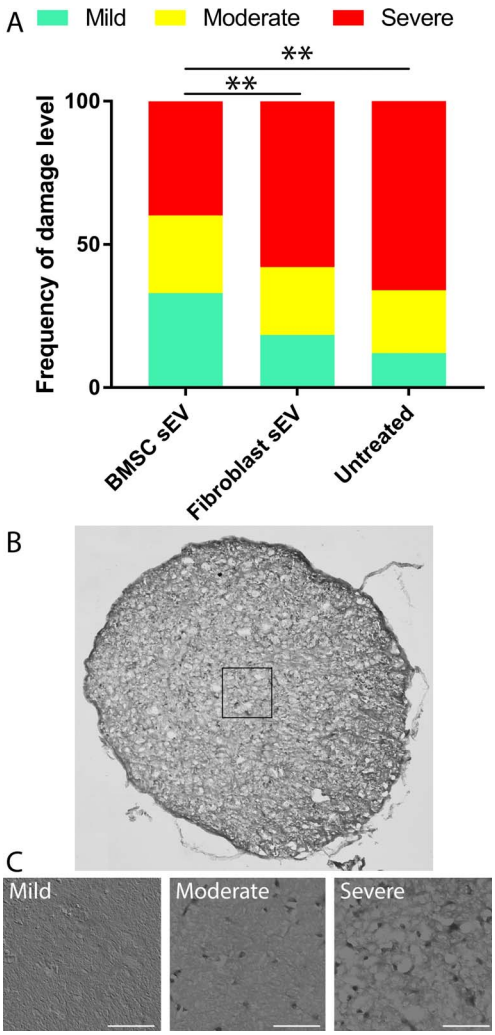

FIGURE 4. Frequency distribution of glaucomatous optic nerve damage in DBA/2J mice. (**A**) Frequency of damage, defined as mild, moderate, or severe and represented as a percentage of the total number of analyzed optic nerve sections from 12-month-old DBA/2J mice with or without *ivit* injection of BMSC- or fibroblast-derived sEV. *Asterisks* indicate significant difference between groups ($P < 0.01$). (**B**) Example of a nerve stained with paraphenylenediamine and a 50 μm × 50 μm box delineating the magnification area for three representative images (**C**) of mild, moderate, and severe classified optic nerve sections (*scale bar*: 15 μm).

quently activated bipolar cells and led to the incorrect incorporation of a partial b-wave along with the pSTR in the amplitude measurements. The functional decline beginning at 6 months, however, mirrors our present findings as well as the scientific consensus that RGC functional decline is an early effect occurring prior to any loss of RGC (reviewed in Refs. 46, 47). One curiosity with these results is the observation that pSTR deficits are seen prior to significant ocular hypertension. One possibility is that IOP had increased but not high or consistently (considering IOP was recorded only once a month) enough to produce a statistical significance. For example, a separate study used a greater number of DBA/2J mice and another technique to record RGC function known as pattern ERG (PERG), which is reported to be more sensitive and is able to detect early deteriorations in RGC function. PERG showed RGC dysfunction beginning after 3 months in DBA/2J mice and was inversely proportional to the rise in IOP, that is, a rise of 1 mm Hg in IOP was seen per month (between ages 2–6 months) with a contemporaneous decrease in PERG amplitude by 1 μV.[27] These increases in 1 mm Hg may have not been detectable in the present study. These PERG experiments demonstrated a complete abolition of responsiveness by 10 to 11 months in DBA/2J mice; however, it is worth noting that PERG amplitudes are reversibly affected by simple postural changes in the DBA/2J mouse.[48]

DBA/2J mice spontaneously developed ocular hypertension with the elevated pressure beginning significantly at 6 months as was also seen in previous studies.[24] This is stereotypical of female DBA/2J mice in comparison to males that develop ocular hypertension beginning significantly at 7–8 months. This is an exaggerated form of normal elevations in IOP as a mouse ages and is followed by deficiencies in axonal transport, functional deterioration, and RGC loss.[24,49] A deterioration in optokinetic response, a visual reflex that allows the eyes to track an object in motion while maintaining a stationary image, has been reported in DBA/2J mice with age/IOP,[49,50] whereas the oculomotor reflex, a similar reflex to optokinetic response but involving movement of the head, is absent even in healthy (>3 month) DBA/2J mice.[26]

Although we did not quantify the number of RGC in healthy DBA/2J mice (<3 months old; prior to any RGC loss), it is well reported that approximately 2750 FluoroGold $(FG)^+$ RGC are found per mm^2 in retinal wholemounts.[51,52] RBPMS stains all major subtypes of RGC and exclusively RGC in the retina.[53] Colocalization experiments show more than 99% of $RBPMS^+$ cells in the retina double label with FG, suggesting that FG^+ and $RBPMS^+$ cell populations in the retina are the same.[54,55] By 12 months, the number of RGC had reduced significantly to less than 300 $RBPMS^+$ RGC per mm^2 in both untreated mice and mice receiving fibroblast-derived sEV, which resembles other studies demonstrating less than 500 FG^+ RGC per mm^2 in 10-month-old DBA/2J mice. About 1000 $RBPMS^+$ RGC per mm^2 survived in the retina of mice receiving BMSC-derived sEV (Fig. 2). Similar survival has been demonstrated with other neuroprotective strategies, for example, ivit transplantation of glial cell line-derived neurotrophic factor (GDNF)-loaded microspheres promoted survival of 1000 to 1500 RGC at similar time points.[51]

Despite the present study injecting human sEV into mice vitreous humor monthly from 3 to 12 months of age, we did not observe any evidence of ocular inflammation. This was largely expected as several studies have demonstrated that transplantation of human MSC does not elicit any inflammatory complications,[56,57] and no difference in the survival of the graft is seen when comparing transplantations of rat MSC into either inbred or outbred rat breeds.[58] Considering that sEV are one small part of MSC and their secretome, the previous data strongly suggest that BMSC-derived sEV do not elicit any kind of inflammatory rejection in the eye.

RGC death in DBA/2J mice is through apoptosis and occurs through a pathway distinct from that responsible for the degeneration of their axons. The knockdown of BAX or JUN prevents loss of RGC, but does not prevent degeneration of their axons.[29,59] Although most control retina were sparsely populated with RGC by 12 months, we did notice that some DBA/2J mice displayed a wedge/patchy pattern of RGC death beginning at the optic nerve head and projecting/widening toward the periphery, as has been described previously.[51] Given the substantial RGC death, this is unlikely to affect the sampling technique used in this study, however, taking an earlier time point may produce much more variably dense retina and may require whole retinal counts for reliability. The regions of RGC death show expression profiles distinct from the nearby unaffected regions.[33] This fan-shaped loss of RGC has been suggested to be explained by a local injury to axonal bundles as they pass through the lamina cribrosa.[34] By using

well-established grading scales to assess optic nerve damage in DBA/2J mice,[24] we demonstrated that mice receiving BMSC-derived sEV performed better on the grading scale, with less nerves being classified as severe and more classified as mild or moderate. Thus, although BMSC-derived sEV are neuroprotective for RGC, they also provide a protective effect on their axons, possibly because the delivery of multiple miRNA via sEV has the potential to interact with multiple neuroprotective pathways that spare the soma and the axon.

In conclusion, the present proof-of-principle study demonstrates efficacy of BMSC sEV during the course of a 1-year period in an animal model of glaucoma. Although all previous studies have been performed using rats and acute models of ocular hypertension, the present study was carried out in mice and during a time period more analogous to the human condition, a necessary step toward clinical testing. Future studies will be directed at further discovering the mechanism of BMSC sEV action in the eye, determining the feasibility of more tolerable administration modalities, and ensuring the safety of sEV treatment into the eye of patients.

Acknowledgments

The authors thank Erin Cullather for her assistance in the optic nerve grading and Richard Libby, PhD, for his advice and guidance in the planning phase of this project.

Supported by the Intramural Research Programs of the National Eye Institute. This project has received funding from the European Union's Horizon 2020 research and innovation program under the Marie Skłodowska-Curie Grant 749346.

Disclosure: **B. Mead**, None; **Z. Ahmed**, None; **S. Tomarev**, None

References

1. Gordon MO, Beiser JA, Brandt JD, et al. The ocular hypertension treatment study: Baseline factors that predict the onset of primary open-angle glaucoma. *Arch Ophthalmol*. 2002;120:714–720.
2. Susanna R, De Moraes CG, Cioffi GA, Ritch R. Why do people (still) go blind from glaucoma? *Trans Vis Sci Tech*. 2015;4(2):1.
3. Mead B, Berry M, Logan A, Scott RAH, Leadbeater W, Scheven BA. Stem cell treatment of degenerative eye disease. *Stem Cell Res*. 2015;14:243–257.
4. Weiss JN, Levy S. Stem cell ophthalmology treatment study: bone marrow derived stem cells in the treatment of retinitis pigmentosa. *Stem Cell Invest*. 2018;5:18–27.
5. Weiss JN, Levy S, Benes SC. Stem cell ophthalmology treatment study: bone marrow derived stem cells in the treatment of non-arteritic ischemic optic neuropathy (naion). *Stem Cell Invest*. 2017;4:94–104.
6. Weiss JN, Levy S, Benes SC. Stem cell ophthalmology treatment study (scots): bone marrow-derived stem cells in the treatment of Leber's hereditary optic neuropathy. *Neural Regen Res*. 2016;11:1685–1694.
7. Satarian L, Nourinia R, Safi S, et al. Intravitreal injection of bone marrow mesenchymal stem cells in patients with advanced retinitis pigmentosa; a safety study. *J Ophthalmic Vis Res*. 2017;12:58–64.
8. Mead B, Logan A, Berry M, Leadbeater W, Scheven BA. Paracrine-mediated neuroprotection and neuritogenesis of axotomised retinal ganglion cells by human dental pulp stem cells: comparison with human bone marrow and adipose-derived mesenchymal stem cells. *PLoS One*. 2014;9:e109305.
9. Johnson TV, Dekorver NW, Levasseur VA, et al. Identification of retinal ganglion cell neuroprotection conferred by platelet-derived growth factor through analysis of the mesenchymal stem cell secretome. *Brain*. 2014;137:503–519.
10. Mead B, Amaral J, Tomarev S. Mesenchymal stem cell–derived small extracellular vesicles promote neuroprotection in rodent models of glaucoma. *Invest Ophthalmol Vis Sci*. 2018;59:702–714.
11. Mead B, Tomarev S. Bmsc-derived exosomes promote survival of retinal ganglion cells through mirna-dependent mechanisms. *Stem Cell Trans Med*. 2017;6:1273–1285.
12. Thery C, Amigorena S, Raposo G, Clayton A. Isolation and characterization of exosomes from cell culture supernatants and biological fluids. *Curr Protoc Cell Biol*. 2006;30:1–29.
13. Valadi H, Ekstrom K, Bossios A, Sjostrand M, Lee JJ, Lotvall JO. Exosome-mediated transfer of mrnas and micrornas is a novel mechanism of genetic exchange between cells. *Nat Cell Biol*. 2007;9:654–659.
14. Keshtkar S, Azarpira N, Ghahremani MH. Mesenchymal stem cell-derived extracellular vesicles: novel frontiers in regenerative medicine. *Stem Cell Res Ther*. 2018;9:63–71.
15. Lankford KL, Arroyo EJ, Nazimek K, Bryniarski K, Askenase PW, Kocsis JD. Intravenously delivered mesenchymal stem cell-derived exosomes target m2-type macrophages in the injured spinal cord. *PLoS One*. 2018;13:e0190358.
16. Sun G, Li G, Li D, et al. Hucmsc derived exosomes promote functional recovery in spinal cord injury mice via attenuating inflammation. *Mater Sci Eng C Mater Biol Appl*. 2018;89:194–204.
17. Wang N, Chen CY, Yang DZ, et al. Mesenchymal stem cells-derived extracellular vesicles, via mir-210, improve infarcted cardiac function by promotion of angiogenesis. *Biochim Biophys Acta Mol Basis Dis*. 2017;1863:2085–2092.
18. Xin H, Li Y, Cui Y, Yang JJ, Zhang ZG, Chopp M. Systemic administration of exosomes released from mesenchymal stromal cells promote functional recovery and neurovascular plasticity after stroke in rats. *J Cereb Blood Flow Metab*. 2013;33:1711–1715.
19. Xin HQ, Katakowski M, Wang FJ, et al. Microrna-17-92 cluster in exosomes enhance neuroplasticity and functional recovery after stroke in rats. *Stroke*. 2017;48:747–753.
20. Jiang-Hu H, Xiao-Ming Y, Yang X, et al. Systemic administration of exosomes released from mesenchymal stromal cells attenuates apoptosis, inflammation, and promotes angiogenesis after spinal cord injury in rats. *J Neurotrauma*. 2017;34:3388–3396.
21. Zhang Y, Chopp M, Liu XS, et al. Exosomes derived from mesenchymal stromal cells promote axonal growth of cortical neurons. *Mol Neurobiol*. 2017;54:2659–2673.
22. Lv Z, Wei Y, Wang D, Zhang CY, Zen K, Li L. Argonaute 2 in cell-secreted microvesicles guides the function of secreted mirnas in recipient cells. *PLoS One*. 2014;9:e103599.
23. Li L, Zhu D, Huang L, et al. Argonaute 2 complexes selectively protect the circulating micrornas in cell-secreted microvesicles. *PLoS One*. 2012;7:e46957.
24. Libby RT, Anderson MG, Pang IH, et al. Inherited glaucoma in DBA/2J mice: Pertinent disease features for studying the neurodegeneration. *Vis Neurosci*. 2005;22:637–648.
25. Turner AJ, Vander Wall R, Gupta V, Klistorner A, Graham SL. DBA/2J mouse model for experimental glaucoma: pitfalls and problems. *Clin Exper Ophthalmol*. 2017;45:911–922.
26. Barabas P, Huang W, Chen H, et al. Missing optomotor head-turning reflex in the DBA/2J mouse. *Invest Ophthalmol Vis Sci*. 2011;52:6766–6773.
27. Saleh M, Nagaraju M, Porciatti V. Longitudinal evaluation of retinal ganglion cell function and IOP in the DBA/2J mouse model of glaucoma. *Invest Ophthalmol Vis Sci*. 2007;48:4564–4572.
28. Salinas-Navarro M, Jimenez-Lopez M, Valiente-Soriano FJ, et al. Retinal ganglion cell population in adult albino and pigmented mice: a computerized analysis of the entire population and its spatial distribution. *Vision Res*. 2009;49:637–647.

Investigative Ophthalmology & Visual Science

29. Libby RT, Li Y, Savinova OV, et al. Susceptibility to neurodegeneration in a glaucoma is modified by bax gene dosage. *PLoS Genetics*. 2005;1:e4.
30. Smith RS. *Systematic Evaluation of the Mouse Eye: Anatomy, Pathology, and Biomethods*. Boca Raton, FL: CRC Press; 2002.
31. Anderson MG, Smith RS, Hawes NL, et al. Mutations in genes encoding melanosomal proteins cause pigmentary glaucoma in DBA/2J mice. *Nat Genet*. 2001;30:81–85.
32. Jakobs TC, Libby RT, Ben Y, John SWM, Masland RH. Retinal ganglion cell degeneration is topological but not cell type specific in DBA/2J mice. *J Cell Biol*. 2005;171:313–325.
33. Panagis L, Zhao X, Ge Y, Ren L, Mittag TW, Danias J. Gene expression changes in areas of focal loss of retinal ganglion cells in the retina of DBA/2J mice. *Invest Ophthalmol Vis Sci*. 2010;51:2024–2034.
34. Howell GR, Libby RT, Jakobs TC, et al. Axons of retinal ganglion cells are insulted in the optic nerve early in DBA/2J glaucoma. *J Cell Biol*. 2007;179:1523–1537.
35. May CA. Comparative anatomy of the optic nerve head and inner retina in non-primate animal models used for glaucoma research. *Open Ophthalmol J*. 2008;2:94–101.
36. Puyang Z, Chen H, Liu X. Subtype-dependent morphological and functional degeneration of retinal ganglion cells in mouse models of experimental glaucoma. *J Nat Sci*. 2015;1:e103.
37. Duan X, Qiao M, Bei F, Kim IJ, He Z, Sanes JR. Subtype-specific regeneration of retinal ganglion cells following axotomy: effects of osteopontin and mtor signaling. *Neuron*. 2015;85:1244–1256.
38. Nassar W, El-Ansary M, Sabry D, et al. Umbilical cord mesenchymal stem cells derived extracellular vesicles can safely ameliorate the progression of chronic kidney diseases. *Biomat Res*. 2016;20:21–31.
39. Kordelas L, Rebmann V, Ludwig AK, et al. Msc-derived exosomes: a novel tool to treat therapy-refractory graft-versus-host disease. *Leukemia*. 2014;28:970–973.
40. Kuriyan AE, Albini TA, Townsend JH, et al. Vision loss after intravitreal injection of autologous "stem cells" for AMD. *N Engl J Med*. 2017;376:1047–1053.
41. Ge QY, Zhou YX, Lu JF, Bai YF, Xie XY, Lu ZH. Mirna in plasma exosome is stable under different storage conditions. *Molecules*. 2014;19:1568–1575.
42. Arroyo JD, Chevillet JR, Kroh EM, et al. Argonaute2 complexes carry a population of circulating microrna independent of vesicles in human plasma. *Proc Natl Acad Sci U S A*. 2011;108:5003–5008.
43. Bogerd HP, Kennedy EM, Whisnant AW, Cullen BR. Induced packaging of cellular microrna into HIV-1 virions can inhibit infectivity. *Mbio*. 2017;8:e02125-16.
44. Klingeborn M, Dismuke WM, Rickman CB, Stamer WD. Roles of exosomes in the normal and diseased eye. *Prog Retinal Eye Res*. 2017;59:158–177.
45. Perez de Lara MJ, Santano C, Guzman-Aranguez A, et al. Assessment of inner retina dysfunction and progressive ganglion cell loss in a mouse model of glaucoma. *Exp Eye Res*. 2014;122:40–49.
46. Porciatti V. Electrophysiological assessment of retinal ganglion cell function. *Exp Eye Res*. 2015;141:164–170.
47. Mead B, Tomarev S. Evaluating retinal ganglion cell loss and dysfunction. *Exp Eye Res*. 2016;151:96–106.
48. Nagaraju M, Saleh M, Porciatti V. IOP-dependent retinal ganglion cell dysfunction in glaucomatous DBA/2J mice. *Invest Ophthalmol Vis Sci*. 2007;48:4573–4579.
49. Yang X-L, van der Merwe Y, Sims J, et al. Age-related changes in eye, brain and visuomotor behavior in the DBA/2J mouse model of chronic glaucoma. *Sci Rep*. 2018;8:4643.
50. Burroughs SL, Kaja S, Koulen P. Quantification of deficits in spatial visual function of mouse models for glaucoma. *Invest Ophthalmol Vis Sci*. 2011;52:3654–3659.
51. Ward MS, Khoobehi A, Lavik EB, Langer R, Young MJ. Neuroprotection of retinal ganglion cells in DBA/2J mice with gdnf-loaded biodegradable microspheres. *J Pharma Sci*. 2007;96:558–568.
52. Zhong L, Bradley J, Schubert W, et al. Erythropoietin promotes survival of retinal ganglion cells in DBA/2J glaucoma mice. *Invest Ophthalmol Vis Sci*. 2007;48:1212–1218.
53. Kwong JM, Caprioli J, Piri N. Rna binding protein with multiple splicing: a new marker for retinal ganglion cells. *Invest Ophthalmol Vis Sci*. 2010;51:1052–1058.
54. Rodriguez AR, Muller LPD, Brecha NC. The RNA binding protein RBPMS is a selective marker of ganglion cells in the mammalian retina. *J Comp Neurol*. 2014;522:1411–1443.
55. Kwong JM, Quan A, Kyung H, Piri N, Caprioli J. Quantitative analysis of retinal ganglion cell survival with rbpms immunolabeling in animal models of optic neuropathies. *Invest Ophthalmol Vis Sci*. 2011;52:9694–9702.
56. Mead B, Hill LJ, Blanch RJ, et al. Mesenchymal stromal cell-mediated neuroprotection and functional preservation of retinal ganglion cells in a rodent model of glaucoma. *Cytotherapy*. 2016;18:487–496.
57. Tan HB, Kang X, Lu SH, Liu L. The therapeutic effects of bone marrow mesenchymal stem cells after optic nerve damage in the adult rat. *Clin Interv Aging*. 2015;10:487–490.
58. Johnson TV, Bull ND, Hunt DP, Marina N, Tomarev SI, Martin KR. Neuroprotective effects of intravitreal mesenchymal stem cell transplantation in experimental glaucoma. *Invest Ophthalmol Vis Sci*. 2010;51:2051–2059.
59. Syc-Mazurek SB, Fernandes KA, Libby RT. Jun is important for ocular hypertension-induced retinal ganglion cell degeneration. *Cell Death Dis*. 2017;8:e2945.

Investigative Ophthalmology & Visual Science